1521-0103/12/3403-638–647$25.00
THE JOURNAL OF PHARMACOLOGY AND EXPERIMENTAL THERAPEUTICS Vol. 340, No. 3
185579/3749581
JPET 340:638–647, 2012

A Fibrinogen-Derived Peptide Provides Intercellular Adhesion Molecule-1-Specific Targeting and Intraendothelial Transport of Polymer Nanocarriers in Human Cell Cultures and Mice[S]

Carmen Garnacho, Daniel Serrano, and Silvia Muro

Institute for Bioscience and Biotechnology Research (C.G., S.M.), Department of Cell Biology and Molecular Genetics and Biological Sciences Graduate Program (D.S.), and Fischell Department of Bioengineering (S.M.), University of Maryland, College Park, Maryland

Received June 27, 2011; accepted November 29, 2011

ABSTRACT

Intercellular adhesion molecule-1 (ICAM-1), a transmembrane glycoprotein expressed on activated endothelium and many other cells, represents a suitable target for delivery of drug nanocarriers (NCs) to disease areas. Numerous works have shown efficient targeting and intracellular transport of ICAM-1-targeted NCs, rendering significant therapeutic potential. This is the case for enzyme delivery for treatment of multitissue lysosomal storage disorders. However, those studies used formulations targeted to ICAM-1 by antibodies (anti-ICAM NCs). This poses an obstacle to preclinical evaluation of long-term treatment of such chronic maladies, caused by immunogenicity of foreign proteins administered to animals, compelling development of alternative strategies. In this work, we used radioisotope tracing, fluorescence and electron microscopy, and in vitro, cell cultures, and mouse models to evaluate polymer nanocarriers targeted to ICAM-1 by a 17-mer linear peptide derived from the ICAM-1-binding sequence of fibrinogen (γ3). Our results show that γ3 NCs target ICAM-1 with efficiency and specificity similar to that of anti-ICAM NCs, determined by using immobilized ICAM-1, native ICAM-1 expressed on endothelial cell cultures, and intravenous administration in mice. Furthermore, γ3 NCs are internalized by cells in culture and in vivo and transported to lysosomes via cell adhesion molecule-mediated endocytosis, without apparent disruption of cell junctions, similar to anti-ICAM counterparts. The degree of conservation of fibrinogen γ3 sequence and its cognate site on ICAM-1 among species (e.g., mouse, chimpanzee, and humans) reflects the interspecies targeting found for γ3 NCs, providing an avenue for exploring the translation of ICAM-1-targeting platforms in the preclinical and, perhaps, future clinical realm.

Introduction

Intercellular adhesion molecule-1 (ICAM-1) is a transmembrane glycoprotein of the Ig superfamily and a coreceptor for leukocyte integrins (Rothlein et al., 1986; Marlin and Springer, 1987). It is predominantly present on the surface of endothelial cells (ECs) and other cell types, and is overexpressed in inflammation, thrombosis, oxidative stress, metabolic diseases, genetic conditions, etc. (reviewed by Muro, 2007 and Hopkins et al., 2004). Hence, ICAM-1 represents a suitable target for helping delivery of drug carriers to areas affected by disease.

Coupling of antibodies against ICAM-1 (anti-ICAM) to the surface of liposomes, microbubbles, or polymer nanocarriers (NCs) has been shown to provide ICAM-1 targeting in cell culture and in vivo (Bloemen et al., 1995; Sakhalkar et al., 2003; Weller et al., 2003; Muro et al., 2005, 2006; Garnacho et al., 2008b; Hsu et al., 2011a, b). For instance, in a rat model of heart transplantation, anti-ICAM contrast microbubbles adhered to the transplanted myocardium attacked by the host immune system, providing ultrasound-mediated detection of acute rejection (Weller et al., 2003). In mouse models of pulmonary pathologies, e.g., acid sphingomyelinase knockout mice mimicking lung dysfunction in type B Niemann-Pick disease, polymer anti-ICAM NCs accumu-

This work was supported by the National Institutes of Health National Heart, Lung and Blood Institute [Grant R01-HL98416] (to S.M.); and the American Heart Association [Grant 09BGIA2450014] (to S.M.).

Article, publication date, and citation information can be found at http://jpet.aspetjournals.org.

http://dx.doi.org/10.1124/jpet.111.185579.

[S] The online version of this article (available at http://jpet.aspetjournals.org) contains supplemental material.

ABBREVIATIONS: ICAM-1, intercellular adhesion molecule-1; CAM, cell adhesion molecule; BSA, bovine serum albumin; EC, endothelial cell; HUVEC, human umbilical vein EC; FITC, fluorescein isothiocyanate; ID, injected dose; NC, nanocarrier; PKC, protein kinase C; PMA, phorbol 12-myristate 13-acetate; TNFα, tumor necrosis factor α; scFV, single-chain Fv construct; VE, vascular endothelial; NHE1, sodium/proton exchanger 1.

lated in this organ, providing enhanced delivery of therapeutics (Garnacho et al., 2008b).

Anti-ICAM-coated drug delivery systems are also endocytosed by cells. This is the case for anti-ICAM liposomes that are rapidly internalized by bronchial epithelial cells in culture (Mastrobattista et al., 1999) or polymer anti-ICAM NCs that are endocytosed by ECs in culture and mice, providing intracellular delivery of therapeutic enzymes (Muro et al., 2008; Hsu et al., 2011a, b).

The internalization pathway of anti-ICAM NCs, cell adhesion molecule (CAM)-mediated endocytosis, is distinct from classic clathrin- and caveolar-mediated pathways, macropinocytosis, and phagocytosis (Muro et al., 2003). In ECs, the most studied example for targeting of anti-ICAM NCs, CAM-mediated endocytosis involves the interaction between ICAM-1 and NHE1, an amiloride-sensitive Na^+/H^+ exchanger that provides linkage to actin stress fibers induced upon binding of anti-ICAM NCs to ECs, signaled through protein kinase C (PKC) (Muro et al., 2003). By this pathway, ECs internalize anti-ICAM NCs from ~200 nm to ~5 μm in diameter, which provides a valuable flexibility of design for ICAM-1-targeted therapeutics (Muro et al., 2008). After internalization, ICAM-1 recycles to the cell surface, whereas anti-ICAM NCs traffic to endosomes and lysosomes (Muro et al., 2005). This enhances the delivery of therapeutic enzymes for the treatment of genetic lysosomal storage disorders, where the relatively ubiquitous distribution of ICAM-1 through the body provides broad enzyme delivery, which is required for treatment of these multiorgan, multitissue diseases (Garnacho et al., 2008b; Muro et al., 2008; Hsu et al., 2011a, b).

However, despite these promising features, further evaluation of the potential clinical translation of ICAM-1-targeting strategies requires the substitution of targeting antibodies by more biocompatible moieties. This is crucial in the case of long-term treatment of chronic maladies, such as the genetic lysosomal storage disorders for which ICAM-1 targeting has proven to be beneficial (Garnacho et al., 2008b; Hsu et al., 2011a, b). Recurrent administration of a foreign and/or relatively large targeting protein [full or truncated IgGs, or recombinant single-chain Fv constructs (scFvs)] may induce immunological and/or inflammatory responses that can confound the interpretation of the potential therapeutic effects and/or pose detrimental side effects (Dempsey et al., 1996; Baiu et al., 1999).

With this in mind, we have started exploring the utility of a short, 17-mer linear peptide derived from a natural ligand of ICAM-1 as a potential targeting moiety for addressing polymer nanocarriers to ICAM-1. This peptide, known as γ3, corresponds to the ICAM-1-binding sequence of the γ chain of human fibrinogen (Altieri et al., 1995), which is involved in strengthening the interaction between macrophages and ECs during inflammation (Languino et al., 1993). Although the ability of γ3 in solution to selectively bind to ICAM-1 expressed on human ECs has been shown (Altieri et al., 1995), its potential to recognize mouse ICAM-1, enabling studies in mouse models in vivo, or its ability to serve as an effective and specific anchor for targeting of relatively bulky nanocarrier particles to cells, have not been tested. In this work, we have examined these aspects by radioisotope tracing and fluorescence and electron microscopy, using in vitro, EC culture, and in vivo models. The results obtained render an optimistic opportunity to advance the design of translational ICAM-1-targeting platforms by using γ3 as an affinity moiety.

Materials and Methods

Antibodies and Reagents. The 17-mer peptide containing the ICAM-1-binding sequence of fibrinogen [γ chain amino acids 117–133: NNQKIVNLKEKVAQLEA (Altieri et al., 1995)], known as γ3, and a peptide containing the corresponding scrambled sequence (γ3S) were synthesized by GenScript (Piscataway, NJ). Chimeric proteins containing human Fc fused to Ig domains 1 and 2 of human or mouse ICAM-1 were from R&D Systems (Minneapolis, MN). Monoclonal antibodies to human or mouse ICAM-1 were R6.5 (Marlin and Springer, 1987) and LB2 (Santa Cruz Biotechnology Inc., Santa Cruz, CA) or YN1 (Jevnikar et al., 1990), respectively. Rabbit polyclonal anti-VE-cadherin was from Santa Cruz Biotechnology Inc. Secondary antibodies were from Jackson ImmunoResearch Laboratories Inc. (West Grove, PA). Fluorescein isothiocyanate (FITC) polystyrene particles (100 nm) were purchased from Polysciences (Warrington, PA). $Na^{125}I$ was from PerkinElmer Life and Analytical Sciences (Waltham, MA), and iodogen was from Thermo Fisher Scientific (Waltham, MA). Cell media and supplements were from Cellgro (Manassas, VA) and Invitrogen (Carlsbad, CA). All other reagents were from Sigma-Aldrich (St. Louis, MO).

Cell Culture. Pooled human umbilical vein ECs (HUVECs; Lonza Walkersville, Inc. (Walkersville, MD) were cultured in M-199 medium supplemented as described previously (Muro et al., 2003). H5V cells, a mouse microvascular EC line, and human embryonic kidney epithelial 293 cells were cultured in Dulbecco's modified Eagle's medium supplemented with 10% fetal bovine serum, 2 mM glutamine, penicillin (100 U/ml), and streptomycin (100 mg/ml). For experiments, cells were seeded on 1% gelatin-coated glass coverslips and activated for 16 h with 10 ng/ml tumor necrosis factor α (TNFα; BD Biosciences, San Jose, CA) to up-regulate ICAM-1 expression as in pathological conditions.

Preparation of Targeted Nanocarriers. For fluorescence and electron microscopy, model polymer nanocarriers were prepared by adsorbing anti-ICAM (clone R6.5 for cell culture experiments and clone YN1 for animal tests), γ3, or control γ3S on the surface of 100 nm-diameter green FITC-labeled polystyrene particles (anti-ICAM NCs, γ3 NCs, or γ3S NCs), as described previously (Muro et al., 2006). When indicated, γ3 NCs contained control nonspecific IgG. For in vivo pharmacokinetics, anti-ICAM, γ3, or γ3S were mixed with tracer amounts of control ^{125}I-IgG (~100–300 nCi), (Muro et al., 2006). Noncoated counterparts were separated by centrifugation, and coated nanocarriers were resuspended by using 1% bovine serum albumin (BSA) in phosphate-buffered saline and sonicated to prevent particle aggregation. The effective diameter of antibody- or peptide-coated particles was ~180 or 130 nm, respectively, measured by dynamic light scattering (Zen3690; Malvern Instruments, Westborough, MA).

Binding of ICAM-1-Targeted Nanocarriers to Immobilized ICAM-1. Purified human or mouse ICAM-1 or BSA control were spotted onto nitrocellulose (200 μg/ml, 5-μl dots). After drying, the membranes were incubated for 15 min at room temperature with FITC-labeled γ3 NCs or anti-ICAM NCs (clones R6.5 or YN1), washed, and imaged by fluorescence microscopy using an Eclipse2000-U (Nikon, Melville, NY), a 60× PlanApo objective, and a FITC filter (Nikon). Images were taken with an ORCA-1CCD camera (Hamamatsu Corporation, Bridgewater, NJ) and analyzed by Image-Pro 3.0 software (Media Cybernetics, Inc., Bethesda, MD) to quantify the number of nanocarriers bound per area.

Binding of ICAM-1-Targeted Nanocarriers to Cells in Culture. Either nonactivated or TNFα-activated, ICAM-1-positive HUVECs or H5V cells, versus ICAM-1-negative 293 cells, were incubated at 37°C for 2 h with FITC-labeled γ3 NCs, γ3S NCs, or anti-ICAM NCs (clone R6.5). After washing off nonbound nanocarriers, cells were fixed in cold 2% paraformaldehyde and imaged by

phase-contrast and fluorescence microscopy using the equipment and software settings described above. Phase-contrast images were used to delimit the cell borders and fluorescence counterparts to then quantify the number of nanocarrier particles bound per cell as described previously (Muro et al., 2006).

To confirm ICAM-1 binding specificity, TNFα-activated HUVECs were preincubated at 4°C for 15 min with control medium or medium containing anti-ICAM (clone LB2), γ3, or γ3S. Then, FITC-labeled γ3 NCs were added to the cells and incubated at 4°C for 30 min. Nonbound particles were washed, cells were fixed, and the relative surface area occupied by γ3 NCs per cell (FITC-positive pixels) was quantified by fluorescence microscopy.

Endocytosis of ICAM-1-Targeted Nanocarriers by Cells. Either nonactivated or TNFα-activated HUVECs were incubated for 1 h at 4°C with green FITC-labeled γ3 NCs containing ~1/3 of the particle surface covered by control IgG. Nonbound nanocarriers were removed and cells were incubated for 1 h at 37°C to permit the internalization of prebound particles. Similar experiments were conducted in the presence of 3 mM amiloride (to inhibit CAM-mediated endocytosis) or 1 μg/ml filipin (to inhibit caveolar pathways) (Muro et al., 2003). After fixation, cells were stained with 4′,6-diamidino-2-phenylindole (to label nuclei), and Texas Red-labeled goat anti-mouse IgG. In the absence of permeabilization, this secondary antibody binds to IgG on the nanocarrier coat only in the case of particles located on the cell surface, but not internalized particles (Muro et al., 2003). Samples were imaged by phase-contrast to delimit the cell borders and fluorescence microscopy to determine the number of nanocarriers internalized per cell (single-labeled green) and that of surface-bound nanocarriers (double-labeled yellow). The internalization percentage was calculated as the fraction of internalized nanocarriers from the total number of nanocarriers associated to cells, as described previously (Muro et al., 2003).

Lysosomal Transport of ICAM-1-Targeted Nanocarriers. TNFα-activated HUVEC lysosomes were labeled by incubating cells with Texas Red dextran (10,000 molecular weight) as described previously (Muro et al., 2005). Cells were then incubated for 2 h at 37°C with FITC-labeled γ3 NCs, to allow binding and endocytosis, followed by removing nonbound nanocarriers and continuing incubation for 1, 2, or 3 h, to allow intracellular traffic. Similar experiments were conducted in the presence of 3 mM amiloride or 0.1 μM phorbol 12-myristate 13-acetate (PMA), which inhibit or activate CAM endocytosis, respectively. After fixation, fluorescence microscopy was used to determine the percentage of FITC nanocarriers that colocalized with Texas Red-labeled lysosomes (Muro et al., 2005).

Effects of ICAM-1-Targeted Nanocarriers on Endothelial Cells. To examine potential fast effects, such as reorganization of the actin cytoskeleton upon binding of γ3 NCs to ECs, TNFα-activated HUVECs were incubated for 30 min at 37°C with green FITC-labeled γ3 NCs, followed by washing, fixation, permeabilization with cold 0.2% Triton X-100, and staining of filamentous actin with red Alexa Fluor 594-labeled phalloidin.

To assess potential delayed effects, such as up-regulation of ICAM-1 expression or disruption of the cell junctions, nonactivated HUVECs were incubated for 5 h at 37°C with FITC-labeled γ3 NCs. After washing and fixation, ICAM-1 was stained by using phycoerythrin (red)-labeled anti-ICAM (clone LB2). Cells were then permeabilized and stained with rabbit anti-VE-cadherin, followed by blue Alexa Fluor 355-labeled goat anti-rabbit IgG. All samples were analyzed by fluorescence microscopy.

Pharmacokinetics and Visualization of ICAM-1-Targeted Nanocarriers in Mice. C57BL/6 mice (The Jackson Laboratory, Bar Harbor, ME) were anesthetized and injected intravenously with 1.8×10^{13} particles/kg of γ3/^{125}I-IgG NCs, γ3S/^{125}I-IgG NCs, anti-ICAM/^{125}I-IgG NCs (anti-ICAM clone YN1), or FITC-labeled nonradioactive counterparts. For studies on pharmacokinetics, blood was collected from the retro-orbital sinus 1, 15, and 30 min after injection, and the liver, lungs, and spleen were collected after euthanasia at the later time point. The ^{125}iodine content of the samples was determined to estimate the percentage of nanocarrier's injected dose (%ID) in circulation or said organs. Similar experiments were performed, where the circulating nanocarriers were removed by perfusion through the left ventricle with phosphate-buffered saline, to eliminate the potential contribution of circulating leukocyte-associated nanocarriers to the fraction of nanocarriers accounted for in organs.

For fluorescence microscopy, circulating nanocarriers were also eliminated by perfusion, followed by fixative (2.5% glutaraldehyde, 4% paraformaldehyde in 0.1 M sodium cacodilate buffer), 30 min after nanocarrier injection. The liver, lungs, and spleen were collected and observed by using a 10× objective as described previously (Garnacho et al., 2008b). For transmission electron microscopy, circulating nanocarriers were perfused by using the reagents described above, 1 h after nanocarrier injection. The lungs were collected and processed as described previously (Garnacho et al., 2008b).

All animal studies were performed according to the *Guide for the Care and Use of Laboratory Animals* (Institute of Laboratory Animal Resources, 1996), as well as Institutional Animal Care and Use Committee-approved protocols and university regulations.

Statistics. Data were calculated as the mean ± S.E.M., where statistical significance was determined by Student's *t* test.

Results

The Fibrinogen-Derived Peptide γ3 Efficiently Targets Nanocarriers to both Human and Mouse ICAM-1. The 17-mer peptide that contains the ICAM-1-binding sequence of the fibrinogen γ chain (NNQKIVNLKEKVAQLEA), known as γ3, has been previously reported to bind specifically to human ICAM-1 (Altieri et al., 1995). To determine whether the peptide can also target polymer nanocarriers to this marker, we coated γ3 on the surface of model FITC-labeled polymer carriers (final diameter ~130 nm) and tested their binding to purified human ICAM-1 immobilized onto nitrocellulose.

Fluorescence microscopy (Fig. 1) showed significant binding of γ3 NCs to human ICAM-1 (4618.0 ± 416.3 NCs/mm^2), which represents a 10.4-fold increase compared with binding of γ3 NCs to control albumin (BSA; 445.6 ± 120.9 NCs/mm^2). Said γ3 NCs also bound to immobilized mouse ICAM-1, even more significantly than to its human counterpart (6034.7 ± 403.9 NCs/mm^2), 1.3-fold over human ICAM-1 and 13.5-fold over control albumin. This is the first time that recognition of

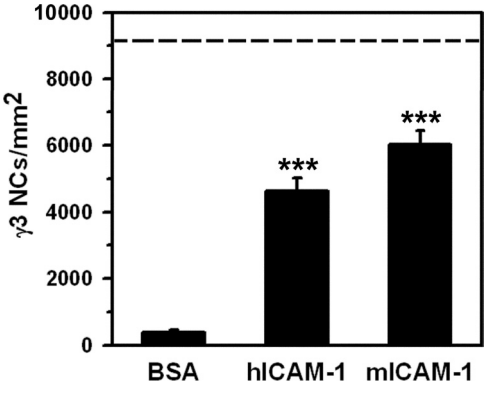

Fig. 1. Binding of γ3-targeted nanocarriers to immobilized ICAM-1. FITC-labeled γ3 NCs (~130 nm) were incubated for 15 min with control BSA, purified human ICAM-1 (hICAM-1), or mouse ICAM-1 (mICAM-1), which had been immobilized on nitrocellulose. The membranes were then washed and analyzed by fluorescence microscopy to quantify the number of nanocarriers bound per area. As a control, ICAM-1 binding of anti-ICAM NCs (clone R6.5) is shown (dashed line). Data are mean ± S.E.M. ($n = 4$). ***, $p < 0.001$, by Student's *t* test (compared with BSA).

mouse ICAM-1 by γ3 has been reported, and this ability of γ3 provides a tool to evaluate the targeting of γ3 NCs in vivo in mouse models. As a comparison, binding of anti-ICAM NCs (clone R6.5) to human ICAM-1 was 9178.2 ± 1086.5 NCs/mm^2, 20.6-fold over control albumin (dashed line in Fig. 1). Hence, the level of binding of γ3 NCs to ICAM-1 was rather relevant: 50.3 ± 4.5% of anti-ICAM NCs in the case of human ICAM-1 and 65.7 ± 4.4% of anti-ICAM NCs for the mouse counterpart. This result further supports the potential targeting utility of γ3 NCs.

As a negative control, we could not detect binding of nanocarriers coated with albumin to either human or mouse ICAM-1 (data not shown).

The γ3 Peptide Specifically Targets Nanocarriers to ICAM-1 Expressed on Human and Mouse Cells. Next, to be able to compare γ3 NCs with anti-ICAM NCs previously characterized in ECs, we determined whether γ3 NCs can also target native ICAM-1 expressed on the surface of these cells in culture. As determined by fluorescence microscopy (Fig. 2A), incubation of FITC-labeled γ3 NCs with activated HUVECs rendered binding of 81.2 ± 4.6 NCs per cell, comparable with the level of binding of control anti-ICAM NCs (95.0 ± 22.1 NCs/cell). No significant binding was found in the case of γ3S NCs (9.2 ± 4.9) or control albumin NCs (data not shown). As reported previously for anti-ICAM NCs (Muro et al., 2003), the level of binding of γ3 NCs was significantly reduced for nonactivated ECs (3.7 ± 0.5-fold reduction; data not shown), as expected because of lower ICAM-1 expression (Muro 2007). In addition, nanocarriers coated with γ3 bound to mouse ECs (H5V) at a level comparable with that of human ECs: 34.8 ± 2.1 NCs/HV5 cell (Fig. 2B), which represents 85.7 to 107.1% the binding found in HUVECs when normalized to the 2- to 2.5-fold larger surface area exposed by the latter cell line. As expected, γ3 NCs did not bind to epithelial 293 cells that lack ICAM-1 expression (8.8 ± 1.9% of HUVECs).

To further confirm specific ICAM-1 targeting by γ3 NCs (Fig. 2C), binding of said nanocarriers to human ECs was tested after treating cells with and in the presence of a monoclonal ICAM-1 antibody (clone LB2) known to block the region of ICAM-1 that binds to γ3 (Altieri et al., 1995). As predicted, anti-ICAM significantly reduced the cell surface area occupied by bound γ3 NCs on ECs (72.3 ± 2.9% reduction). In addition, excess γ3 peptide free in solution competed binding of γ3 NCs (51.8 ± 3.3% reduction), which was specific compared with treatment of cells with a peptide containing the γ3 sequence in scrambled order (γ3S; 13.6 ± 3.4% reduction).

Altogether, this set of experiments further supports the results obtained in the case of binding of γ3 NCs to immobilized proteins, confirming the relative efficiency and specificity of targeting of γ3 NCs to cells expressing ICAM-1.

Nanocarriers Targeted to Cells by γ3 Peptide Are Endocytosed and Transported Intracellularly via the CAM-Mediated Pathway. Cells internalize nanocarriers coated with anti-ICAM via CAM-mediated endocytosis, historically characterized by using ECs (Muro et al., 2003). Hence, we tested whether γ3 NCs can be internalized by these cells in a similar manner.

For this purpose, we first used an established multiple-fluorescence microscopy technique (see *Materials and Methods*) that allows differential identification of surface-bound nanocarriers (double-labeled yellow particles) versus internalized nanocarriers (single-labeled green particles) (Muro et al., 2003). As shown in Fig. 3A, a marked fraction of all γ3 NCs associated to activated ECs was internalized after 1 h (71.1 ± 2.1% uptake), which is comparable with previously reported values for anti-ICAM NCs (ranging from ~70 to 90%; Muro et al., 2003; Hsu et al., 2011b). As expected, the

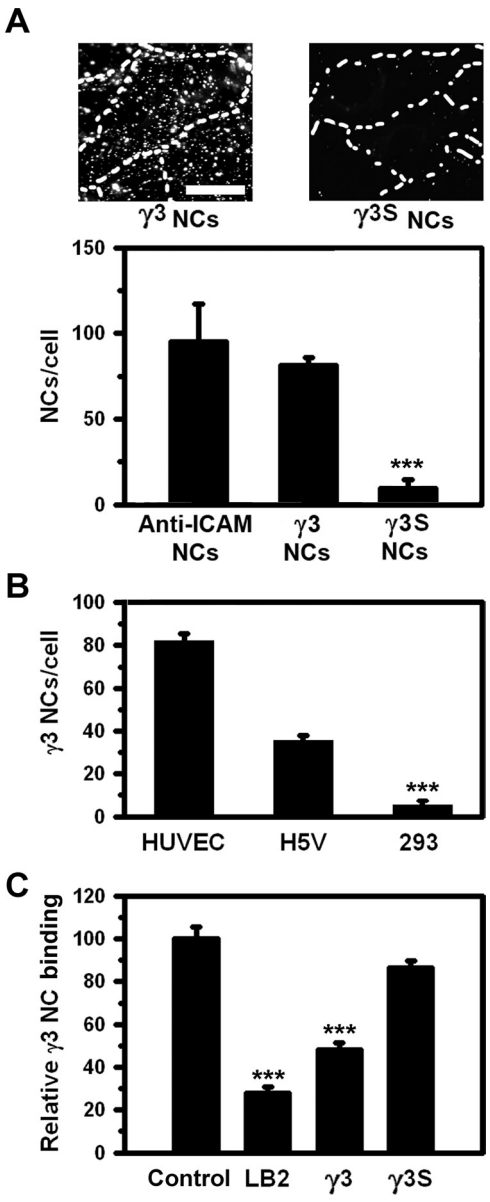

Fig. 2. Binding of γ3-targeted nanocarriers to cells in culture. A, TNFα-activated HUVECs were incubated for 2 h at 37°C with either FITC-labeled anti-ICAM NCs (clone R6.5), γ3 NCs, or γ3S NCs then washed, fixed, and analyzed by fluorescence microscopy. Examples for fluorescence micrographs comparing γ3 NCs with γ3S NCs are shown. Dashed lines mark cell borders, determined by phase-contrast. Scale bar, 10 μm. B, binding of FITC-labeled γ3 NCs to mouse endothelial cells (TNFα-activated H5V cells) and epithelial cells that lack ICAM-1 (TNFα-activated 293 cells) was compared with that of binding to human endothelial cells (TNFα-activated HUVECs). C, TNFα-activated HUVECs were preincubated for 30 min at 4°C with control medium or medium containing anti-ICAM antibody LB2, γ3 peptide, or nonspecific γ3S. FITC-labeled γ3 NCs were then added to the cells and incubated for 30 min at 4°C, and binding was analyzed after washing nonbound particles, using fluorescence microscopy to determine the cell surface area (pixels) occupied by carriers. Results were normalized to the control samples. Data are mean ± S.E.M. ($n \geq 25$ cells, two experiments). ***, $p < 0.001$, by Student's t test [compared with anti-ICAM NCs (A) of HUVEC controls (B)].

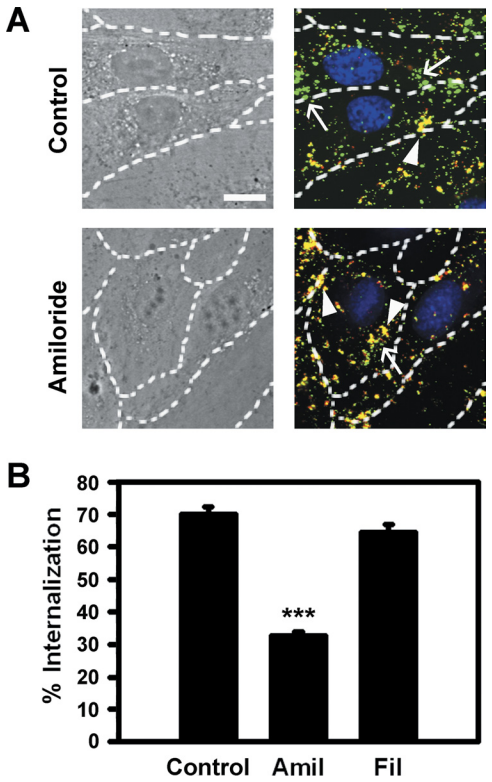

Fig. 3. Endocytosis of γ3-targeted nanocarriers by endothelial cells. TNFα-activated HUVECs were incubated with FITC-labeled γ3/IgG NCs for 1 h at 4°C to permit binding, then washed and incubated for 1 h at 37°C to allow internalization. Experiments were conducted in control medium or medium containing 3 mM amiloride (Amil) to inhibit CAM-mediated endocytosis or 1 μg/ml filipin (Fil) to inhibit caveolar-mediated uptake. After fixation, samples were stained with Texas Red goat anti-mouse IgG, which can bind only to IgG cocoated on γ3/IgG NCs that are located on the cell surface, but not their internalized counterparts. Nuclei were labeled with 4′,6-diamidino-2-phenylindole. A, phase-contrast and merged fluorescence micrographs show internalized γ3/IgG NCs as single-labeled green particles (arrows) versus surface-bound double-labeled (yellow) counterparts (arrowheads). Dashed lines mark cell borders, determined by phase-contrast. Scale bar, 10 μm. B, internalization was quantified as the percentage of internalized γ3/IgG NCs relative to total number of particles associated to cells. Data are mean ± S.E.M. ($n \geq 25$ cells, two experiments). ***, $p < 0.001$, by Student's t test (compared with control).

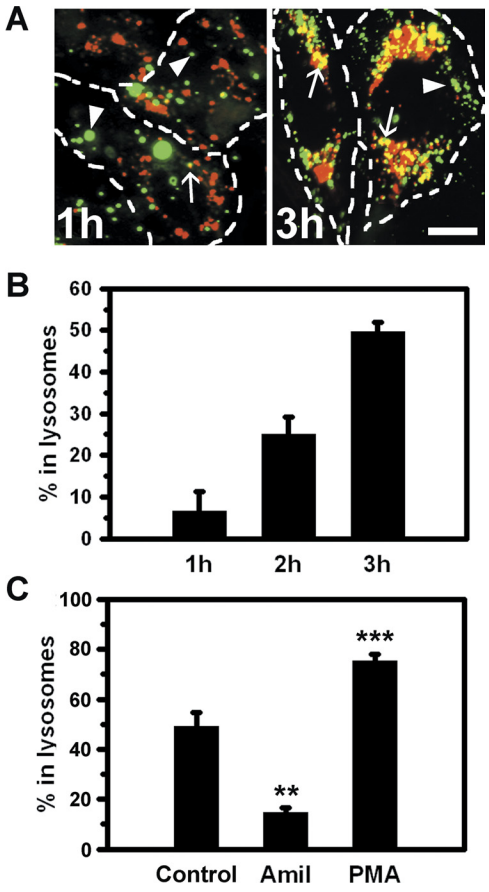

Fig. 4. Lysosomal transport of γ3-targeted nanocarriers in endothelial cells. A, TNFα-activated HUVECs were incubated for 1 h at 37°C with Texas Red dextran to label lysosomes, followed by washing and incubation of cells with FITC-labeled γ3 NCs for 2 h at 37°C to allow binding and uptake (pulse). After washing, cells were incubated for 1, 2, or 3 h (chase), and then fixed. Merged fluorescence microscopy images show green carriers that do not colocalize with red lysosomes (arrowheads) versus lysosomal-located particles (yellow; arrows). Dashed lines mark cell borders, determined by phase-contrast. Scale bar, 10 μm. B, the percentage of lysosomal colocalization of γ3 NCs is shown. C, similar experiments (3-h chase) were conducted in the presence of control cell medium or medium containing 3 mM amiloride to inhibit CAM-mediated endocytosis or 0.1 μM PMA to enhance this pathway via PKC activation. Colocalization of FITC-green γ3 NCs with Texas Red dextran-labeled lysosomes was assessed by fluorescence microscopy as in B. Data are mean ± S.E.M. ($n \geq 25$ cells; two experiments). **, $p < 0.01$; ***, $p < 0.001$, by Student's t test (compared with control).

absolute amount of γ3 NCs internalized per cell was markedly reduced in the case of nonactivated ECs (55.5 ± 6.5% of activated cells; data not shown). However, the efficacy of internalization was not reduced (116.0 ± 8.2% of activated cells; data not shown), as previously observed for anti-ICAM NCs (Muro et al., 2003).

Internalization of γ3 NCs was significantly inhibited by amiloride (51.9 ± 1.7% reduction; Fig. 3), an agent that inhibits ion exchanger proteins, such as NHE1 involved in CAM-mediated endocytosis (Muro et al., 2003). As a negative control, filipin, an agent that affects cholesterol and inhibits caveolar-mediated endocytosis, did not affect internalization of γ3 NCs by ECs (91.8 ± 3.3% of control; Fig. 3B). Thus, these results suggest that, as previously observed for anti-ICAM NCs (Muro et al., 2003), γ3 NCs are also internalized by cells via CAM-mediated endocytosis.

Confirming this (Fig. 4, A and B), γ3 NCs also followed the intracellular route described for anti-ICAM NCs (Muro et al., 2005; Hsu et al., 2011b). Using fluorescence microscopy we found that, after an initial 2-h pulse-incubation period to allow sufficient binding to and endocytosis of γ3 NCs by ECs, nanocarrier particles colocalized with Texas Red dextran-labeled lysosomes in a time-dependent manner: only a minor fraction of γ3 NCs colocalized with lysosomes 1 h after the initial pulse-incubation (6.7 ± 4.6%), but this increased to 25.1 ± 4.4% by 2-h and 49.8 ± 5.8% by 3-h chase-incubation periods. Lysosomal colocalization of γ3 NCs within ECs was significantly affected by amiloride (66.2 ± 5.2% reduction; Fig. 4C), in agreement with NHE1-dependent CAM-mediated endocytosis. In addition, activation of PKC by PMA, which is known to stimulate CAM-mediated endocytosis (Muro et al., 2003), resulted in an increased transport of γ3 NCs to lysosomes (158.4 ± 5.2% of control cells), further confirming the pathway of intraendothelial transport of these carriers.

Effects of γ3-Targeted Nanocarriers on Endothelial Cell Status. Engagement of ICAM-1 on ECs has been shown to induce signaling cascades leading to cytoskeletal changes,

increased endothelial permeability, regulation of gene expression, and other outcomes (Marlin and Springer, 1987; Hopkins et al., 2004; Muro 2007). We evaluated whether such type of responses were induced by γ3 NCs.

Fluorescence microscopy showed that binding of γ3 NCs to ECs resulted in a marked reorganization of the actin cytoskeleton, with formation of stress fibers across the EC body (Fig. 5A and Supplemental Fig. 1A). This is in accord to and needed for effective progression of CAM-mediated endocytosis (Muro et al., 2003). In addition, engagement of endothelial ICAM-1 by γ3 NCs led to a modest, yet statistically significant, stimulation of ICAM-1 expression in ECs (1.8 ± 0.2-fold increase; Fig. 5B and Supplemental Fig. 1B). This is in agreement with a reported role of ICAM-1 in inducing expression of cell adhesion molecules, including its own expression (Hopkins et al., 2004; Muro, 2007). However, these changes did not result in disruption of the cell junctions, as observed by examination of the distribution of VE-cadherin (Fig. 5C and Supplemental Fig. 1C), as observed previously in the case of anti-ICAM NCs (Garnacho et al., 2008b; Muro et al., 2008).

Nanocarriers Targeted to Endothelial ICAM-1 by γ3 Peptide Efficiently Target and Are Internalized by the Endothelium In Vivo. Based on the similar targeting, intracellular transport, and effects observed for γ3 NCs compared with anti-ICAM NCs in vitro and in cell cultures, we examined these peptide-targeted nanocarriers in vivo.

Anti-ICAM NCs have been reported to predominantly target the lung of C57BL/6 mice after intravenous injection, because this organ receives the whole venous cardiac output and is associated with relatively high ICAM-1 expression (Muro et al., 2005; Garnacho et al., 2008b; Hsu et al., 2011b). In agreement with this, accumulation of γ3 NCs in the lung was 54.6 ± 4.5% of the ID (30 min after injection; Fig. 6A), significantly higher than in the liver (17.9 ± 2.7% ID) or spleen (2.0 ± 0.3% ID; data not shown), two organs associated with blood clearance by the reticuloendothelial system. In contrast, γ3S NCs predominantly accumulated in the liver (42.9 ± 5.7%) versus the lung (10.9 ± 1.1% ID). Accumulation in the spleen was also modest for γ3S NCs (3.7 ± 2.3; data not

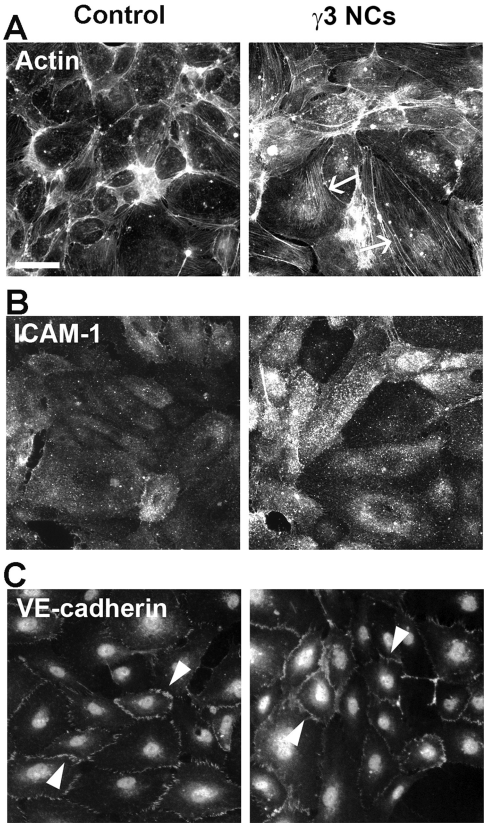

Fig. 5. Effects of γ3-targeted NCs on endothelial cells. A, TNFα-activated HUVECs were incubated for 30 min at 37°C in the absence (control) or presence of γ3/IgG NCs. Cells were then washed, fixed, permeabilized, and stained with Alexa Fluor 594-labeled phalloidin to visualize F-actin. Arrows mark the presence of actin stress fibers. B and C, nonactivated HUVECs were incubated for 5 h at 37°C in the absence (control) or presence of γ3/IgG NCs. B, surface ICAM-1 was immunostained after cell fixation by using phycoerythrin-labeled anti-ICAM (clone LB2). C, endothelial adherens junctions were immunostained after cell fixation and permeabilization, using rabbit anti-VE-cadherin followed by an Alexa Fluor 355-labeled goat anti-rabbit IgG. Arrowheads mark cell-cell junctions. Scale bar, 40 μm.

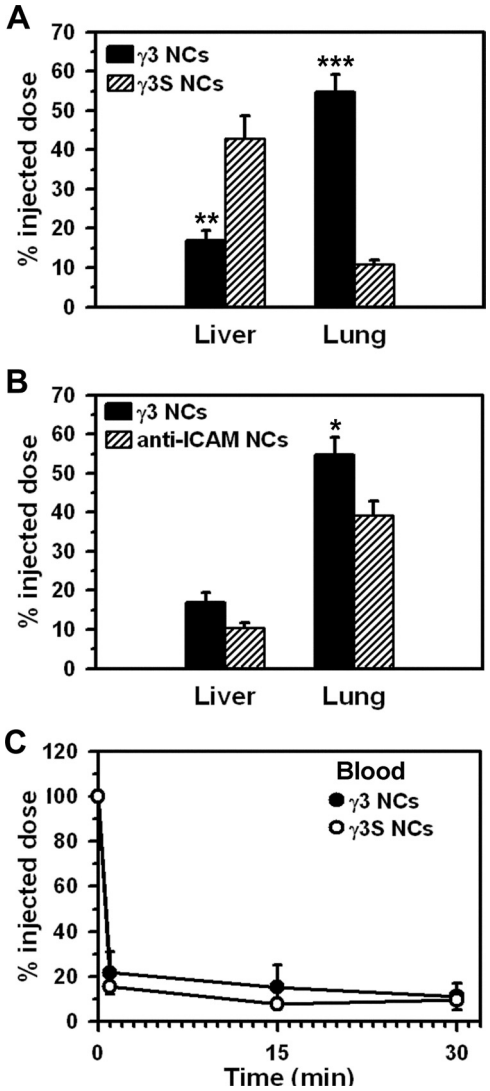

Fig. 6. Pharmacokinetics of γ3-targeted nanocarriers in mice. A, anesthetized C57BL/6 mice were injected intravenously with γ3/^{125}I-IgG NCs or nonspecific control γ3S/^{125}I-IgG NCs. The level of the carriers accumulated in liver and lung was assessed 30 min after injection and expressed as the percentage of the ID (%ID). B, accumulation of γ3/^{125}I-IgG NCs in the liver and lung was compared with that of anti-ICAM NCs (clone YN1). C, the circulating level of carriers, assessed at 1 to 2, 15, and 30 min after injection, is shown. Data are mean ± S.E.M. ($n \geq 3$ mice). Asterisks compare γ3 NCs to γ3S NCs (A) and γ3 NCs to anti-ICAM NCs (B). *, $p < 0.05$; **, $p < 0.01$; ***, $p < 0.001$, by Student's t test.

shown). These biodistribution patterns are similar to that of anti-ICAM NCs versus control IgG NCs reported previously (Muro et al., 2005; Garnacho et al., 2008b; Hsu et al., 2011b), suggesting specific ICAM-1 targeting by γ3 NCs. Indeed, compared with anti-ICAM NCs, γ3 NCs showed a similar biodistribution pattern (Fig. 6B), with even somewhat enhanced lung targeting (54.6 ± 4.5% for γ3 NCs versus 39.2 ± 3.7% ID for anti-ICAM NCs). Further validating ICAM-1 specificity, γ3 NCs did not accumulate in the lungs in ICAM-1 knockout mice (11.8 ± 2.8% ID; data not shown).

In contrast to accumulation of γ3 NCs in the lung (54.6 ± 4.5% ID; Fig. 6A), only 11.5 ± 2.8% ID was found in the total body blood fraction by 30 min (Fig. 6C). Nonspecific control γ3S NCs were similarly eliminated from the circulation, with only 9.7 ± 0.4% ID in the blood 30 min after injection. This elimination from the blood is similar to that of anti-ICAM NCs and control IgG NCs (Muro et al., 2006; Hsu et al., 2011b) and indicates a minimal, if any, contribution of ICAM-1 targeting of circulating cells (e.g., ICAM-1-positive leukocytes). Validating this, the circulation pattern of γ3 NCs in ICAM-1 knockout mice was statistically similar to that of control mice (5.6 ± 1.4% ID at 30 min; data not shown). In addition, intracardiac perfusion to eliminate the circulating fraction of γ3 NCs did not reduce the level of carriers detected in the lung (84.4 ± 3.9% of the nonperfused fraction comparing %ID, or 120.4 ± 14.3% of the nonperfused counterpart comparing %ID per g of lung, to account for the different weight of these samples; data not shown).

We then verified the presence of γ3 NCs in organs by fluorescence microscopy of postmortem specimens, which were collected 30 min after intravenous injection of nanocarriers and imaged after eliminating by perfusion the nanocarrier circulating fraction. As shown in Fig. 7A, γ3 NCs markedly appeared in the lungs and were also visible in the liver and, more modestly, the spleen, in accord to radioisotope tracing experiments.

Finally, transmission electron microscopy of postmortem specimens collected 1 h after intravenous injection of γ3 NCs showed nanocarrier particles bound to the surface of pulmonary ECs, in regions where clathrin pits (invagination marked by the pound sign in Fig. 7B) or caveoli were absent (arrowhead in Fig. 7B, top). Nanocarrier particles were also found within pulmonary ECs (arrow in Fig. 7B, bottom), suggesting internalization of γ3 NCs by the endothelium in vivo as shown previously for anti-ICAM NCs (Garnacho et al., 2008b; Muro et al., 2008). Nanocarrier particles seemed to be contained within membranous compartments that do not present a clathrin coat and were larger and morphologically distinct from classic caveoli. For instance, nanocarriers appeared as ~110- to 120-nm ovoid-shaped objects due to typical nanocarrier deformation during sectioning, versus ~60- to 70-nm spherical omega-shaped vesicles that presented a neck diaphragm (invaginations marked by asterisks in Fig. 7B), which have been described to be morphological features of caveoli (Stan, 2005).

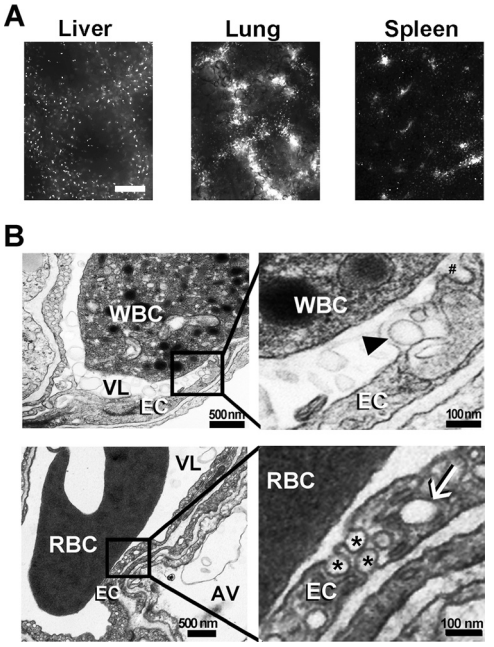

Fig. 7. Visualization of γ3-targeted nanocarriers in mice. A, fluorescence microscopy of mouse liver, lungs, and spleen 30 min after injection with γ3 NCs. Scale bar, 100 μm. B, transmission electron microscopy of mouse lungs 1 h after injection with γ3 NCs. The right pictures (scale bar, 100 nm) represent magnified areas of the left pictures (scale bar, 500 nm). The arrowhead marks a carrier particle bound on a pulmonary EC. The arrow marks a carrier particle internalized by a pulmonary EC. RBC, red blood cell; VL, vascular lumen; AV, alveolus. ∗, caveoli. #, clathrin-coated pit.

Discussion

Although antibodies represent valuable tools to establish proof-of-principle for targeted drug delivery strategies, full IgGs contain Fc fragments, which can induce the formation of immune complexes capable of binding to Fc and/or complement receptors on the surface of antigen-presenting cells, also leading to generation of long-lasting immunity (Dempsey et al., 1996; Baiu et al., 1999). Therefore, future preclinical evaluation of the translational utility of ICAM-1-targeted NCs in the context of treatment for chronic maladies compels substitution of current targeting antibodies (anti-ICAM) by more biocompatible affinity moieties. Generation of anti-ICAM fragments by enzymatic cleavage of IgGs or production of recombinant scFvs have been proven to be valuable alternatives to the use of full antibody molecules (Huston et al., 1993; Nishimura et al., 1996; Saito et al., 2000). However, these antibody-derived sequences still represent foreign and relatively large proteins (scFvs are ≥25–30 kDa), which may contain epitopes that can be recognized by the immune system in long-term applications.

A strategy to overcome this obstacle is that of the use of short-affinity peptides. In this work, we focused on a 17-mer linear peptide, γ3, derived from one of the natural ligands of ICAM-1: fibrinogen (Languino et al., 1993; Altieri et al., 1995). This peptide corresponds to the sequence of the γ chain of human fibrinogen that binds to human ICAM-1 (Altieri et al., 1995). However, γ3 has never been tested in the context of targeting drug delivery carriers to ICAM-1-expressing cells. This is not a trivial issue, because it has been previously shown that even monoclonal antibodies known to bind with relatively good affinity to cell adhesion molecules can fail to target polymer nanocarriers to these markers, likely due to steric hindrance imposed by the carrier particle (Garnacho et al., 2008a). Our results in this work demonstrate that this approach is possible in the case of ICAM-1 targeting by γ3, which may be due at least in part to

the fact that γ3 binds to a membrane-distal domain on the ICAM-1 molecule (D'Souza et al., 1996), avoiding potential accessibility problems of more membrane-proximal epitopes. Indeed, compared with NCs targeted via antibodies that recognize membrane-distal domains of ICAM-1 (antibodies R6.5 and YN1), γ3 NCs showed similar efficiency and specificity when tested for binding against the purified immobilized target (Fig. 1), native ICAM-1 expressed on EC cultures (Fig. 2), or the pulmonary endothelium in mice (Fig. 6).

Also similar to anti-ICAM NCs, γ3 NCs were internalized by ECs both in cell culture (Fig. 3) and in vivo (Fig. 7), and were subsequently trafficked to lysosomes (Fig. 4). This transport was mediated by the CAM-mediated pathway (as in the case of anti-ICAM NCs), as deducted from the formation of actin stress fibers associated to this route (Fig. 5) and the fact that it was reduced by amiloride, which inhibits NHE1 involved in this pathway (Muro et al., 2003), and enhanced by phorbol esters that activate PKC, also involved in CAM-mediated endocytosis (Muro et al., 2003). This property of internalization and subsequent lysosomal transport of γ3 NCs by cells was also unpredictable despite our results indicating that these carriers bind well to ICAM-1. For instance, in another work we found that among a battery of similar polymer nanocarriers, each one targeted via a different antibody but all of them recognizing the same cell adhesion molecule (platelet-endothelial cell adhesion molecule 1), some carriers induced endocytosis in ECs, whereas one nanocarrier did not, despite the fact that all showed similar binding to a membrane-distal epitope of their target molecule (Garnacho et al., 2008a). In addition, among the internalized nanocarriers, a particular antibody-targeted formulation trafficked to lysosomes, whereas another one did not (Garnacho et al., 2008a).

Hence, the fact that γ3 NCs followed this pathway was rather serendipitous, yet it provides the possibility of exploring this approach for intracellular drug delivery. Lysosomal trafficking of γ3 NCs suggests the suitability of this strategy in the context of lysosomal enzyme therapies. This is the case for delivery of acid sphingomyelinase, α-galactosidase, or α-glucosidase, which are deficient in types A-B Niemann-Pick disease, Fabry disease, or Pompe disease, respectively, where ICAM-1 expression by multiple cells in the body favored enzyme delivery in these multiorgan, multitissue diseases, previously tested for anti-ICAM NCs (Garnacho et al., 2008b; Muro et al., 2008; Hsu et al., 2011a, b). Furthermore, transport to acidic lysosomal compartments could theoretically provide controlled drug release, e.g., by pH-responsive carriers (Stayton et al., 2005).

It is noteworthy that γ3 NCs recognized both human and mouse ICAM-1 (Figs. 1, 2, and 5), which represents a key finding to further study the utility of this targeting strategy both in human cell cultures and in vivo murine models, as shown in this work. This feature of γ3 to present species cross-reactivity had not been reported previously, yet is in agreement with the level of conservation of its cognate sequence in the ICAM-1 molecule between these two species. The region of ICAM-1 to which γ3 binds is located in the first Ig domain, between amino acids 8 to 21 of the mature protein (D'Souza et al., 1996). As shown in Fig. 8, 57.1% of the residues in this region are identical between human and mouse, 21.4% are conserved substitutions, and 14.2% are semiconserved changes. In addition, there is a high degree of

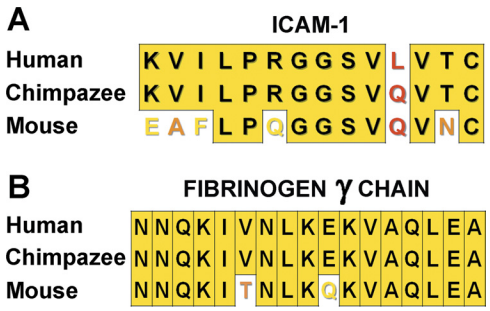

Fig. 8. Degree of conservation of ICAM-1 (8–21) and γ fibrinogen (117–133) sequences among species. A, comparison of the region of ICAM-1 to which γ3 binds (amino acids 8–21 in the human counterpart) among human (Swiss-Prot accession number P05362), chimpanzee (Swiss-Prot accession number Q28806), and mouse (Swiss-Prot accession number P13597) ICAM-1. B, comparison of the γ3 sequence of fibrinogen γ chain (amino acids 117–133 in the human counterpart) for human (Swiss-Prot accession number P02679), chimpanzee (National Center for Biotechnology Information accession number XP_00113878.1), and mouse (Swiss-Prot accession number Q8VCM7). Yellow boxes show identical amino acid residues compared with human sequences, amino acid residues marked in yellow correspond to conserved substitutions, those marked in orange correspond to semiconserved changes, and residues marked in red are nonconserved changes.

conservation in the γ3 sequence of the fibrinogen γ chain between human and mouse (88.2% identical residues and 5.9% conserved substitutions). This species cross-reactivity also represents a valuable tool for obtaining data on ICAM-1-targeting strategies not only in mice, but also in large-scale animals, including nonhuman primates. As an example, the fibrinogen binding region of ICAM-1 in the chimpanzee has only one single residue change compared with its human counterpart. This may enable preclinical evaluation and optimization of ICAM-1-targeting platforms based on γ3, and further clinical trials, because this peptide recognizes human ICAM-1.

Several other ICAM-1 affinity peptides have been generated in the past. For instance, this is the case for several peptides developed by using phage display techniques to block leukocyte-endothelial adhesion or intercellular adhesion of immune cells during antigen presentation (Welply et al., 1996; Bélizaire et al., 2003). However, these peptides were specifically selected to recognize mouse ICAM-1, hence whether they can recognize its human counterpart or are suitable for targeting of drug delivery carriers to cells remains unknown.

Another set of interesting ICAM-1-targeting peptides are those derived, as in our work, from molecules that can bind to ICAM-1, such as certain sequences derived from MUC1 mucin core proteins (Hayashi et al., 2001), P(0) CAM (Jaafari and Foldvari, 2002), cyclic peptides derived from the $\alpha_L\beta_2$ integrin, leukocyte functional antigen-1 (Anderson and Siahaan, 2003; Sillerud et al., 2004). Most of these peptides have also been developed and tested in the context of blocking ICAM-1-mediated adhesion during inflammation and cancer metastasis and have been shown to bind to human ICAM-1 but have not been tested in other species. Arguably, the most interesting example of such a peptide from the perspective of targeting drug delivery systems to ICAM-1 is cLABL, which has been shown to provide efficient binding to human epithelial and endothelial cells (Zhang et al., 2008; Chittasupho et al., 2009). The species cross-reactivity of this peptide, en-

abling preclinical animal testing, and its ability to induce endocytosis and lysosomal transport are unknown.

It is noteworthy that several properties of the γ3 peptide may provide advantages to this γ3-mediated ICAM-1-targeting strategy. For instance, fibrinogen forms a molecular bridge strengthening the adhesion between endothelial ICAM-1 and the leukocyte integrin $\alpha_M\beta_2$ (Mac-1) during inflammation (Languino et al., 1993). As a consequence, binding of γ3 (the fibrinogen region that provides attachment to ICAM-1) to ICAM-1 has been shown to decrease inflammation (Altieri et al., 1995). It has been also postulated that γ3 may attenuate atherosclerosis (Altieri et al., 1995) and ICAM-1-dependent infections (Hopkins et al., 2004), and γ3 promotes cell survival and antiapoptotic effects in activated ECs (Duperray et al., 1997; Gardiner and D'Souza, 1999; Pluskota and D'Souza, 2000). The fact that binding of γ3 NCs only modestly enhances ICAM-1 expression on nonactivated ECs with no apparent disruption of the cell junctions (Fig. 5) suggests a relative safety of this strategy. Yet, there is potential for side effects by targeting ICAM-1 with this peptide for drug delivery purposes, and this will need to be explored thoroughly in endothelial and other ICAM-1-positive cell types. An important example is that of T cells, where ICAM-1 is involved in the immunological synapse and, hence, its blockage may cause modulation of the immune response, as observed in the case of other peptides (Chittasupho et al., 2011; Manikwar et al., 2011).

Altogether, the results reported in this work show that model polymer nanocarriers coated with γ3 efficiently and specifically bind to both human and mouse ICAM-1. This provides targeting and intracellular transport similar to that of anti-ICAM NCs reported previously, offering a new opportunity to advance the design of translational ICAM-1-targeting platforms.

Acknowledgments

We thank members of the University of Pennsylvania Biomedical Imaging Core (Philadelphia, PA) and the University of Maryland Nanocenter and the Laboratory for Biological Ultrastructure (College Park, MD) for technical assistance regarding transmission electron microscopy.

Authorship Contributions

Participated in research design: Garnacho and Muro.

Conducted experiments: Garnacho and Serrano.

Performed data analysis: Garnacho, Serrano, and Muro.

Wrote or contributed to the writing of the manuscript: Garnacho and Muro.

References

Altieri DC, Duperray A, Plescia J, Thornton GB, and Languino LR (1995) Structural recognition of a novel fibrinogen γ chain sequence (117–133) by intercellular adhesion molecule-1 mediates leukocyte-endothelium interaction. *J Biol Chem* **270:**696–699.

Anderson ME and Siahaan TJ (2003) Mechanism of binding and internalization of ICAM-1-derived cyclic peptides by LFA-1 on the surface of T cells: a potential method for targeted drug delivery. *Pharm Res* **20:**1523–1532.

Baiu DC, Prechl J, Tchorbanov A, Molina HD, Erdei A, Sulica A, Capel PJ, and Hazenbos WL (1999) Modulation of the humoral immune response by antibody-mediated antigen targeting to complement receptors and Fc receptors. *J Immunol* **162:**3125–3130.

Bélizaire AK, Tchistiakova L, St-Pierre Y, and Alakhov V (2003) Identification of a murine ICAM-1-specific peptide by subtractive phage library selection on cells. *Biochem Biophys Res Commun* **309:**625–630.

Bloemen PG, Henricks PA, van Bloois L, van den Tweel MC, Bloem AC, Nijkamp FP, Crommelin DJ, and Storm G (1995) Adhesion molecules: a new target for immunoliposome-mediated drug delivery. *FEBS Lett* **357:**140–144.

Chittasupho C, Siahaan TJ, Vines CM, and Berkland C (2011) Autoimmune therapies targeting costimulation and emerging trends in multivalent therapeutics. *Ther Deliv* **2:**873–889.

Chittasupho C, Xie SX, Baoum A, Yakovleva T, Siahaan TJ, and Berkland CJ (2009) ICAM-1 targeting of doxorubicin-loaded PLGA nanoparticles to lung epithelial cells. *Eur J Pharm Sci* **37:**141–150.

Dempsey PW, Allison ME, Akkaraju S, Goodnow CC, and Fearon DT (1996) C3d of complement as a molecular adjuvant: bridging innate and acquired immunity. *Science* **271:**348–350.

D'Souza SE, Byers-Ward VJ, Gardiner EE, Wang H, and Sung SS (1996) Identification of an active sequence within the first immunoglobulin domain of intercellular cell adhesion molecule-1 (ICAM-1) that interacts with fibrinogen. *J Biol Chem* **271:**24270–24277.

Duperray A, Languino LR, Plescia J, McDowall A, Hogg N, Craig AG, Berendt AR, and Altieri DC (1997) Molecular identification of a novel fibrinogen binding site on the first domain of ICAM-1 regulating leukocyte-endothelium bridging. *J Biol Chem* **272:**435–441.

Gardiner EE and D'Souza SE (1999) Sequences within fibrinogen and intercellular adhesion molecule-1 (ICAM-1) modulate signals required for mitogenesis. *J Biol Chem* **274:**11930–11936.

Garnacho C, Albelda SM, Muzykantov VR, and Muro S (2008a) Differential intra-endothelial delivery of polymer nanocarriers targeted to distinct PECAM-1 epitopes. *J Control Release* **130:**226–233.

Garnacho C, Dhami R, Simone E, Dziubla T, Leferovich J, Schuchman EH, Muzykantov V, and Muro S (2008b) Delivery of acid sphingomyelinase in normal and Niemann-Pick disease mice using intercellular adhesion molecule-1-targeted polymer nanocarriers. *J Pharmacol Exp Ther* **325:**400–408.

Hayashi T, Takahashi T, Motoya S, Ishida T, Itoh F, Adachi M, Hinoda Y, and Imai K (2001) MUC1 mucin core protein binds to the domain 1 of ICAM-1. *Digestion* **63 (Suppl 1):**87–92.

Hopkins AM, Baird AW, and Nusrat A (2004) ICAM-1: targeted docking for exogenous as well as endogenous ligands. *Adv Drug Deliv Rev* **56:**763–778.

Hsu J, Northrup L, Bhowmick T and Muro S (2011a) Delivery of α-glucosidase for Pompe disease by ICAM-1-targeted polymer nanocarriers. *Nanomed-Nanotechnol* http://dx.doi.org/10.1016/j.nano.2011.08.014.

Hsu J, Serrano D, Bhowmick T, Kumar K, Shen Y, Kuo YC, Garnacho C, and Muro S (2011b) Enhanced endothelial delivery and biochemical effects of α-galactosidase by ICAM-1-targeted nanocarriers for Fabry disease. *J Control Release* **149:**323–331.

Huston JS, Tai MS, McCartney J, Keck P, and Oppermann H (1993) Antigen recognition and targeted delivery by the single-chain Fv. *Cell Biophys* **22:**189–224.

Institute of Laboratory Animal Resources (1996) *Guide for the Care and Use of Laboratory Animals* 7th ed. Institute of Laboratory Animal Resources, Commission on Life Sciences, National Research Council, Washington DC.

Jaafari MR and Foldvari M (2002) Targeting of liposomes to human keratinocytes through adhesive peptides from immunoglobulin domains in the presence of IFN-γ. *Drug Deliv* **9:**1–9.

Jevnikar AM, Wuthrich RP, Takei F, Xu HW, Brennan DC, Glimcher LH, and Rubin-Kelley VE (1990) Differing regulation and function of ICAM-1 and class II antigens on renal tubular cells. *Kidney Int* **38:**417–425.

Languino LR, Plescia J, Duperray A, Brian AA, Plow EF, Geltosky JE, and Altieri DC (1993) Fibrinogen mediates leukocyte adhesion to vascular endothelium through an ICAM-1-dependent pathway. *Cell* **73:**1423–1434.

Manikwar P, Kiptoo P, Badawi AH, Buyuktimkin B, and Siahaan TJ (2011) Antigen-specific blocking of CD4-specific immunological synapse formation using BPI and current therapies for autoimmune diseases. *Med Res Rev* http://dx.doi.org/10.1002/med. 20243.

Marlin SD and Springer TA (1987) Purified intercellular adhesion molecule-1 (ICAM-1) is a ligand for lymphocyte function-associated antigen 1 (LFA-1). *Cell* **51:**813–819.

Mastrobattista E, Storm G, van Bloois L, Reszka R, Bloemen PG, Crommelin DJ, and Henricks PA (1999) Cellular uptake of liposomes targeted to intercellular adhesion molecule-1 (ICAM-1) on bronchial epithelial cells. *Biochim Biophys Acta* **1419:**353–363.

Muro S (2007) Intercellular adhesion molecule-1 and vascular cell adhesion molecule-1, in *Endothelial Biomedicine* (Aird WC ed) pp 1058–1070, Cambridge University Press, New York.

Muro S, Dziubla T, Qiu W, Leferovich J, Cui X, Berk E, and Muzykantov VR (2006) Endothelial targeting of high-affinity multivalent polymer nanocarriers directed to intercellular adhesion molecule 1. *J Pharmacol Exp Ther* **317:**1161–1169.

Muro S, Gajewski C, Koval M, and Muzykantov VR (2005) ICAM-1 recycling in endothelial cells: a novel pathway for sustained intracellular delivery and prolonged effects of drugs. *Blood* **105:**650–658.

Muro S, Garnacho C, Champion JA, Leferovich J, Gajewski C, Schuchman EH, Mitragotri S, and Muzykantov VR (2008) Control of endothelial targeting and intracellular delivery of therapeutic enzymes by modulating the size and shape of ICAM-1-targeted carriers. *Mol Ther* **16:**1450–1458.

Muro S, Wiewrodt R, Thomas A, Koniaris L, Albelda SM, Muzykantov VR, and Koval M (2003) A novel endocytic pathway induced by clustering endothelial ICAM-1 or PECAM-1. *J Cell Sci* **116:**1599–1609.

Nishimura Y, Takei Y, Kawano S, Goto M, Nagano K, Tsuji S, Nagai H, Ohmae A, Fusamoto H, and Kamada T (1996) The F(ab')2 fragment of an anti-ICAM-1 monoclonal antibody attenuates liver injury after orthotopic liver transplantation. *Transplantation* **61:**99–104.

Pluskota E and D'Souza SE (2000) Fibrinogen interactions with ICAM-1 (CD54) regulate endothelial cell survival. *Eur J Biochem* **267:**4693–4704.

Rothlein R, Dustin ML, Marlin SD, and Springer TA (1986) A human intercellular adhesion molecule (ICAM-1) distinct from LFA-1. *J Immunol* **137:**1270–1274.

Saito K, Fujii K, Awazu Y, Nakayamada S, Nakano K, Aso M, Ota T, and Tanaka Y (2000) Intercellular adhesion molecule-1 (ICAM-1) mediated gene delivery to rheu-

matoid synovial cells using the Fab fragments of anti-ICAM-1 monoclonal antibody. *Nihon Rinsho Meneki Gakkai Kaishi* **23:**533–537.

Sakhalkar HS, Dalal MK, Salem AK, Ansari R, Fu J, Kiani MF, Kurjiaka DT, Hanes J, Shakesheff KM, and Goetz DJ (2003) Leukocyte-inspired biodegradable particles that selectively and avidly adhere to inflamed endothelium in vitro and in vivo. *Proc Natl Acad Sci U S A* **100:**15895–15900.

Sillerud LO, Burks EJ, Brown WM, Brown DC, and Larson RS (2004) NMR solution structure of a potent cyclic nonapeptide inhibitor of ICAM-1-mediated leukocyte adhesion produced by homologous amino acid substitution. *J Pept Res* **64:**127–140.

Stan RV (2005) Structure of caveolae. *Biochim Biophys Acta* **1746:**334–348.

Stayton PS, El-Sayed ME, Murthy N, Bulmus V, Lackey C, Cheung C, and Hoffman AS (2005) 'Smart' delivery systems for biomolecular therapeutics. *Orthod Craniofac Res* **8:**219–225.

Weller GE, Lu E, Csikari MM, Klibanov AL, Fischer D, Wagner WR, and Villanueva FS (2003) Ultrasound imaging of acute cardiac transplant rejection with microbubbles targeted to intercellular adhesion molecule-1. *Circulation* **108:**218–224.

Welply JK, Steininger CN, Caparon M, Michener ML, Howard SC, Pegg LE, Meyer DM, De Ciechi PA, Devine CS, and Casperson GF (1996) A peptide isolated by phage display binds to ICAM-1 and inhibits binding to LFA-1. *Proteins* **26:**262–270.

Zhang N, Chittasupho C, Duangrat C, Siahaan TJ, and Berkland C (2008) PLGA nanoparticle–peptide conjugate effectively targets intercellular cell-adhesion molecule-1. *Bioconjug Chem* **19:**145–152.

Address correspondence to: Silvia Muro, Institute for Bioscience and Biotechnology Research, University of Maryland, 5115 Plant Sciences Building, College Park, MD 20742-4450. E-mail: muro@umd.edu